



## Particle motion nearby rough surfaces

Christina Kurzthaler <sup>1</sup>, Lailai Zhu <sup>1,2,3</sup>, Amir A. Pahlavan <sup>1</sup>, and Howard A. Stone <sup>1,\*</sup>

<sup>1</sup>*Department of Mechanical and Aerospace Engineering, Princeton University, New Jersey 08544, USA*

<sup>2</sup>*Department of Mechanical Engineering, National University of Singapore, 117575, Singapore*

<sup>3</sup>*Linné Flow Centre and Swedish e-Science Research Centre (SeRC), KTH Mechanics, SE-10044 Stockholm, Sweden*



(Received 8 April 2020; accepted 27 July 2020; published 17 August 2020)

We study the hydrodynamic coupling between particles and solid, rough boundaries characterized by random surface textures. Using the Lorentz reciprocal theorem, we derive analytical expressions for the grand mobility tensor of a spherical particle and find that roughness-induced velocities vary nonmonotonically with the characteristic wavelength of the surface. In contrast to sedimentation near a planar wall, our theory predicts continuous particle translation transverse and perpendicular to the applied force. Most prominently, this motion manifests itself in a variance of particle displacements that grows quadratically in time along the direction of the force. This increase is rationalized by surface roughness generating particle sedimentation closer to or farther from the surface, which entails a significant variability of settling velocities.

DOI: [10.1103/PhysRevFluids.5.082101](https://doi.org/10.1103/PhysRevFluids.5.082101)

Particle sedimentation in low-Reynolds-number flows represents a fundamental problem in physics and fluid dynamics and has been studied over decades due to its relevance for natural and technological applications. These range from the separation of multicomponent systems on the microscale [1,2] to macroscopic geological phenomena [3]. Confining geometries omnipresent in natural environments and microfluidic devices, however, significantly alter the sedimentation process due to long-range hydrodynamic interactions [4–7]. Unlike planar surfaces, these boundaries display a large variety of structured and rough topographies with random heterogeneities, which modify the surrounding flow fields [8–12] and hydrodynamically impact nearby particle motion [13,14]. Understanding the physical mechanisms underlying the interactions of the particles with these boundaries lays the foundation for the design of novel particle separation methods [15–17] and tools for the noninvasive measurement of surface properties reminiscent of microrheology [18,19].

A rigid spherical particle that sediments nearby a vertical planar wall does not translate perpendicular to the wall and thus keeps a constant distance to it [20,21]. This behavior, however, changes drastically for spheroidal particles and slender rods, whose anisotropic shape generates intricate tumbling behavior [22,23], and in the presence of fluid inertia [24,25] or near elastic boundaries [26], which can both induce a lift force and generate particle migration away from the surface. The impact of complex surface shapes has only been studied for particles suspended in shear flow near periodic surfaces that can induce motion across streamlines [14,27,28]. Despite its ubiquity, however, the hydrodynamic coupling between sedimenting particles and rough surfaces with random features remains an open question at the interface of low-Reynolds-number flows and statistical physics.

Here, we study hydrodynamic interactions between a sphere and a textured surface and provide an analytic expression for the particle mobility. We employ our theory to elucidate the motion of a

---

\*[hastone@princeton.edu](mailto:hastone@princeton.edu)

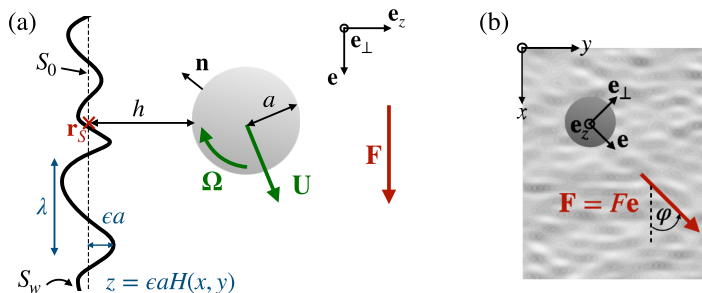


FIG. 1. (a) Side view of a sphere with radius  $a$  near a vertical rough wall  $S_w$ , characterized by the shape function  $H(x, y)$ , a wavelength  $\lambda$ , and amplitude  $\epsilon a$ . In response to an external force  $\mathbf{F} = F \mathbf{e}$  (parallel to  $S_0$ ), the sphere translates and rotates with velocities  $\mathbf{U}$  and  $\mathbf{\Omega}$ , respectively. The sphere is located at  $\mathbf{r}_S$  and at a distance  $h$  relative to  $S_0$ . (b) Top view of the sphere and the rough surface (grayscale indicates a height map), where  $x, y$  are the coordinates spanning  $S_0$ . Here,  $\mathbf{F}$  is oriented at an angle  $\varphi$  relative to the surface structure and  $\mathbf{e}, \mathbf{e}_\perp$ , and  $\mathbf{e}_z$  denote the unit vectors along, transverse, and perpendicular to  $\mathbf{F}$ .

sedimenting sphere near a rough surface with random features and find that the velocities depend nonmonotonically on the characteristic wavelength of the surface. In contrast to sedimentation near a planar wall, the particle translates perpendicular and transverse to the applied force. Our study reveals that these hydrodynamic interactions generate a variability in settling velocities and thereby induce a variance of the particle displacements along the force direction that displays a quadratic increase at long times. We further relate the particle mobility to the spatially dependent diffusivity of a Brownian particle.

*Model.* We consider the motion of a spherical particle with radius  $a$  in an incompressible flow of a viscous fluid nearby a rough surface,  $S_w$ , in three dimensions (3D) [Fig. 1]. The quasisteady fluid velocity  $\mathbf{u}(\mathbf{r})$  and pressure fields  $p(\mathbf{r})$  are described by the continuity and Stokes equations,  $\nabla \cdot \mathbf{u} = 0$  and  $\nabla \cdot \boldsymbol{\sigma} = \mathbf{0}$ , with stress field  $\boldsymbol{\sigma} = -p\mathbb{I} + \mu(\nabla \mathbf{u} + \nabla \mathbf{u}^T)$  and viscosity  $\mu$ . In the comoving frame of reference that is attached to the sphere, the no-slip boundary conditions (BCs) are  $\mathbf{u} = \mathbf{\Omega} \wedge \mathbf{r}$  on  $S_p$  and  $\mathbf{u} = -\mathbf{U}$  on  $S_w$  and  $S_\infty$ , which denotes the bounding surface at infinity. The instantaneous translational and rotational velocities of the sphere,  $\mathbf{U} = \mathbf{U}(\mathbf{r}_S, h)$  and  $\mathbf{\Omega} = \mathbf{\Omega}(\mathbf{r}_S, h)$ , depend on its distance from the wall,  $h = h(t)$ , its position,  $\mathbf{r}_S = \mathbf{r}_S(t)$ , relative to the underlying surface, which determines the particle velocities locally, and time  $t$ .

We describe the small height fluctuations of the textured surface by  $z = \epsilon a H(x, y)$ , where  $H(x, y)$  denotes the shape function and  $\epsilon a$  the surface amplitude with dimensionless parameter  $\epsilon \ll 1$ . Assuming that the surface amplitude is smaller than the particle-wall distance,  $\epsilon a \ll h$ , we expand the velocity field in  $\epsilon$ ,  $\mathbf{u} = \mathbf{u}^{(0)} + \epsilon \mathbf{u}^{(1)} + \mathcal{O}(\epsilon^2)$ . Equivalently, we express the translational and rotational velocities of the sphere by  $\mathbf{U} = \mathbf{U}^{(0)} + \epsilon \mathbf{U}^{(1)} + \mathcal{O}(\epsilon^2)$  and  $\mathbf{\Omega} = \mathbf{\Omega}^{(0)} + \epsilon \mathbf{\Omega}^{(1)} + \mathcal{O}(\epsilon^2)$ . Using the method of domain perturbation, we express the no-slip BC at the rough surface  $S_w$  in terms of a Taylor expansion about  $z = 0$  (surface  $S_0$ ). The expansion enables us to consider the zeroth- and first-order problems separately with BCs,  $\mathbf{u}^{(0)} = -\mathbf{U}^{(0)}$ , and

$$\mathbf{u}^{(1)} = -\mathbf{U}^{(1)} - aH(x, y) \frac{\partial \mathbf{u}^{(0)}}{\partial z} \Big|_{z=0} \quad \text{on } S_0, \quad (1)$$

which contains a roughness-induced slip velocity [8–10] dictated by the zeroth-order flow and the surface shape.

Then the zeroth-order problem with flow field  $\mathbf{u}^{(0)}$  corresponds to a sphere moving near a planar wall which has been elaborated analytically in terms of a bispherical representation [29–32]. The first-order correction to the fluid flow,  $\mathbf{u}^{(1)}$ , encodes details of the rough surface. It obeys the Stokes and continuity equations with BCs:  $\mathbf{u}^{(1)} = \mathbf{\Omega}^{(1)} \wedge \mathbf{r}$  on  $S_p$ ,  $\mathbf{u}^{(1)} = -\mathbf{U}^{(1)}$  on  $S_\infty$ , and Eq. (1). In creeping flow, the total force and torque exerted on the particle are zero. Here, the applied force  $\mathbf{F}$

and torque  $\mathbf{L}$  are balanced by the hydrodynamic force and torque of the zeroth-order problem,  $\mathbf{F}_H^{(0)} = \int_{S_p} \mathbf{n} \cdot \boldsymbol{\sigma}^{(0)} dS$  and  $\mathbf{L}_H^{(0)} = \int_{S_p} \mathbf{r} \wedge (\mathbf{n} \cdot \boldsymbol{\sigma}^{(0)}) dS$ , where the normal vector  $\mathbf{n}$  is directed away from  $S_p$ . Consequently, the sphere in the first-order problem is force and torque free, which determines its roughness-induced velocities.

*Particle mobility.* We develop an analytic theory for the mobility of a sphere near a rough wall by employing the Lorentz reciprocal theorem, which relates two Stokes flow problems that share the same geometry but have different boundary conditions [33,34]. We introduce as the auxiliary problem,  $\hat{\mathbf{u}}, \hat{\boldsymbol{\sigma}}$ , the flow generated by a moving sphere near a planar wall. The Lorentz reciprocal theorem relates it to the first-order problem with velocity field  $\mathbf{u}^{(1)}$  and stresses  $\boldsymbol{\sigma}^{(1)}$  via

$$\int_{S_p, S_0, S_\infty} \mathbf{n} \cdot \boldsymbol{\sigma}^{(1)} \cdot \hat{\mathbf{u}} dS = \int_{S_p, S_0, S_\infty} \mathbf{n} \cdot \hat{\boldsymbol{\sigma}} \cdot \mathbf{u}^{(1)} dS. \quad (2)$$

Since the first-order problem is force and torque free, the left-hand side of Eq. (2) vanishes. We insert the BCs of the main and auxiliary problems into Eq. (2) and note that by the divergence theorem the hydrodynamic force on the sphere in the auxiliary problem obeys  $\hat{\mathbf{F}}_H = - \int_{S_0, S_\infty} \mathbf{n} \cdot \hat{\boldsymbol{\sigma}} dS$ . Thus, Eq. (2) simplifies to

$$\hat{\mathbf{F}}_H \cdot \mathbf{U}^{(1)} + \hat{\mathbf{L}}_H \cdot \boldsymbol{\Omega}^{(1)} = \int_{S_0} aH(x, y) \mathbf{n} \cdot \hat{\boldsymbol{\sigma}} \cdot \left. \frac{\partial \mathbf{u}^{(0)}}{\partial z} \right|_{z=0} dS. \quad (3)$$

Due to the linearity of the Stokes equations and the rigid boundaries of the particle and the wall, the particle velocities must be coupled linearly to the applied force and torque via the grand mobility tensor  $\mathbf{M}$ ,  $(\mathbf{U}, \boldsymbol{\Omega})^T = \mathbf{M} \cdot (\mathbf{F}, \mathbf{L})^T$  [33]. Its components encode the coupling between the translational and rotational velocities with the forces and torques,  $\mathbf{M}_{UF}$  and  $\mathbf{M}_{\Omega L}$ , respectively, and between the rotation and force (translation and torque),  $\mathbf{M}_{\Omega F}$  ( $\mathbf{M}_{UL}$ ). We further expand the mobility tensor in terms of the small roughness parameter  $\epsilon$ ,  $\mathbf{M} = \mathbf{M}^{(0)} + \epsilon \mathbf{M}^{(1)} + \mathcal{O}(\epsilon^2)$ , where  $\mathbf{M}^{(0)}$  is the mobility of a sphere near a planar wall and  $\mathbf{M}^{(1)}$  corresponds to the roughness-induced mobility. Since the velocity field and stresses are linear in the forces and torques, we arrive at the general form for the grand mobility tensor [see Supplemental Material (SM) [35]]

$$\mathbf{M} = \mathbf{M}^{(0)} - \epsilon \int_{S_0} aH(x, y) \mathbf{K} dS + \mathcal{O}(\epsilon^2), \quad (4)$$

which accounts for the influence of surface topography. The coupling tensor  $\mathbf{K}$  can be assumed known as it depends on the zeroth-order problem only. The grand mobility tensor represents an exact result up to second order in  $\epsilon$  determined by the (arbitrary) surface shape and the instantaneous position of the sphere,  $\mathbf{M}[\mathbf{r}_s(t), h(t); H]$ . The linearity of the Stokes equations and the rigid boundaries entail that  $\mathbf{M}$  is symmetric and positive definite [36].

We note that the analytical theory is valid for low-Reynolds-number flows and small surface roughness with  $\text{Re} \lesssim \epsilon \lesssim 1$ . For  $\text{Re} \sim \epsilon$  our theory needs to be modified to account for inertial effects “in the spirit of Saffman” that could generate migration away from the wall [24].

Subsequently, we investigate the sedimentation of a sphere in response to a force  $\mathbf{F}$  near a random, rough wall. We use the exact bispherical representation of the fluid flow  $\mathbf{u}^0$  to calculate the coupling tensor  $\mathbf{K}$  and evaluate the velocities,  $\mathbf{U} = \mathbf{M}_{UF} \cdot \mathbf{F}$  and  $\boldsymbol{\Omega} = \mathbf{M}_{\Omega F} \cdot \mathbf{F}$ , via numerical integration. We validated our analytical solutions for a periodic surface with a boundary integral method that captures the full surface shape (see SM [35]).

*Roughness-induced velocities.* We describe the random rough wall by a statistical framework [37]. The surface shape is modeled as a superposition of  $N \times N$  Fourier modes with random amplitudes  $\alpha_{nm}, \beta_{nm}$ ,

$$H(\mathbf{r}_0) = \frac{1}{N} \sum_{n,m=1}^N \alpha_{nm} \sin(\mathbf{k}_m^n \cdot \mathbf{r}_0) + \beta_{nm} \cos(\mathbf{k}_m^n \cdot \mathbf{r}_0), \quad (5)$$

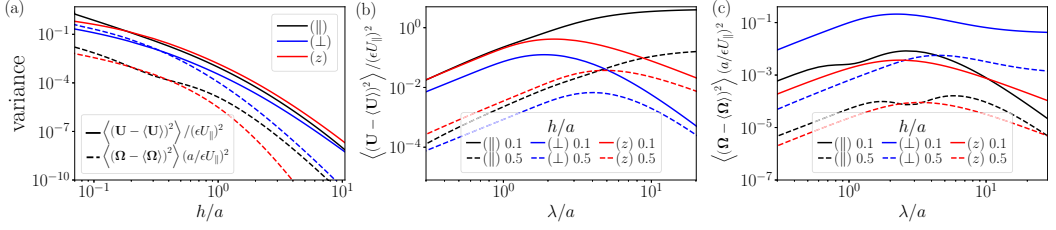


FIG. 2. Variance of the translational,  $\langle (\mathbf{U} - \langle \mathbf{U} \rangle)^2 \rangle$ , and rotational velocities,  $\langle (\mathbf{\Omega} - \langle \mathbf{\Omega} \rangle)^2 \rangle$ , with respect to (a) the distance  $h/a$  with  $\lambda/a = 2$  and (b), (c) the wavelength  $\lambda/a$ . (b) and (c) show the variances for different particle-surface distances,  $h/a = 0.1, 0.5$ . Here,  $U_{\parallel}$  denotes the settling velocity of a sphere near a planar wall and we have used  $N = 50$  in Eq. (5). The variances are shown for the velocities along ( $\parallel$ ), transverse ( $\perp$ ), and perpendicular ( $z$ ) to the force direction,  $\mathbf{F} = F \mathbf{e}_x$ .

where  $\mathbf{r}_0 \in S_0$ ,  $\mathbf{k}_m^n = (k_n, k_m)^T$  with  $k_j = 2\pi j / (\lambda N)$ , and wavelength  $\lambda$ . The amplitudes are statistically independent, random normal variables with zero mean and unit variance. The height fluctuations vanish on average,  $\langle H \rangle = 0$ , and display a variance,  $\langle (\epsilon a H)^2 \rangle = (\epsilon a)^2$ , where  $\langle \cdot \rangle$  is the average over all surface realizations.

The applied force,  $\mathbf{F} = F \mathbf{e}$ , is directed parallel to  $S_0$  but can be oriented with respect to the surface structure [Fig. 1(b)]. Then roughness-induced velocities are decomposed into components parallel, transverse, and perpendicular to it,  $\mathbf{U}^{(1)} = U_{\parallel}^{(1)} \mathbf{e}_{\parallel} + U_{\perp}^{(1)} \mathbf{e}_{\perp} + U_z^{(1)} \mathbf{e}_z$  with  $\mathbf{e}_{\perp} = \mathbf{e}_z \wedge \mathbf{e}$  and similarly  $\mathbf{\Omega}^{(1)}$ . They are determined by the local geometry of the underlying random surface and therefore we are interested in average quantities. Since the velocities depend linearly on the surface shape, the average velocities remain independent of the roughness and reduce to that of a sphere near a planar wall,  $\langle \mathbf{U} \rangle = \mathbf{U}^{(0)} = U_{\parallel} \mathbf{e}$  and  $\langle \mathbf{\Omega} \rangle = \mathbf{\Omega}^{(0)} = \Omega^{(0)} \mathbf{e}_{\perp}$ , where  $\Omega^{(0)}$  is related to  $U_{\parallel}$ . The settling velocity decreases for decreasing  $h/a$  due to the wall-induced extra hydrodynamic drag and is obtained via the balance of gravitational and hydrodynamic forces,  $U_{\parallel} \sim \ln(a/h)^{-1}$  (for  $h/a \lesssim 1$ ) [20]. The sphere rotates to balance the hydrodynamic torque arising from the presence of the wall [21].

The velocity fluctuations due to the surface roughness become apparent in the variance of the translational velocities, which grows quadratically to leading order in  $\epsilon$ ,  $\langle (\mathbf{U} - \langle \mathbf{U} \rangle)^2 \rangle = \epsilon^2 \langle (\mathbf{U}^{(1)})^2 \rangle + \mathcal{O}(\epsilon^3)$  (see SM [35]). They are determined by the particle-wall distance  $h/a$  and wavelength of the surface  $\lambda/a$ . The translational velocity fluctuations decay roughly eight orders in magnitude for  $0.1 \lesssim h/a \lesssim 10$  [Fig. 2(a)], which indicates that for increasing  $h/a$  transport is governed by the average wall contribution. We note that the velocity fluctuations transverse to the force are smaller than perpendicular to it. The variance of the rotational velocities,  $\langle (\mathbf{\Omega} - \langle \mathbf{\Omega} \rangle)^2 \rangle = \epsilon^2 \langle (\mathbf{\Omega}^{(1)})^2 \rangle + \mathcal{O}(\epsilon^3)$ , decays even faster and remains most pronounced for rotation around  $\mathbf{e}_{\perp}$ .

Most prominently, the variances of the perpendicular,  $\langle (U_z^{(1)})^2 \rangle$ , and transverse velocities,  $\langle (U_{\perp}^{(1)})^2 \rangle$ , display a maximum at a characteristic wavelength  $\lambda_{\max}$  [Fig. 2(b)]. This nonmonotonic behavior can be rationalized as for  $\lambda \lesssim \lambda_{\max}$  the surface area closest to the particle contains several heterogeneities with steep slopes that smear out roughness-induced flows and therefore the velocity fluctuations perpendicular and transverse to the force vanish. In contrast, for  $\lambda \gtrsim \lambda_{\max}$  the particle experiences the presence of a smooth wall as the surface slope becomes negligible and thus the roughness-induced velocities decrease. We also find that  $\lambda_{\max}$  for  $h/a = 0.5$  is  $\sim 2$  times larger than for  $h/a = 0.1$ , because larger flows are required to transmit information of the roughness to a particle that is located further away and these are generated in larger cavities.

Differently, the velocity fluctuations along the force,  $\langle (U_{\parallel}^{(1)})^2 \rangle$ , saturate for large  $\lambda$ , where the surface appears almost flat [Fig. 2(b)] but is shifted a small amount closer to or farther away from the sphere. Then the settling velocity of a sphere near a wall that is  $\epsilon a$  closer to or farther away, provides an upper bound of the variance  $[U_{\parallel}(h/a \pm \epsilon) - U_{\parallel}(h/a)]^2 \sim (\epsilon a/h)^2 U_{\parallel}(h/a)^2$  (for  $h/a \lesssim 1$ ).

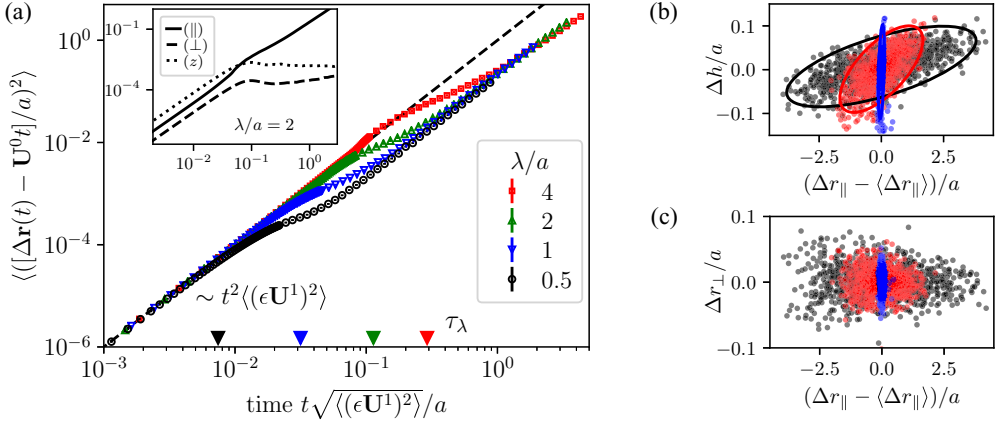


FIG. 3. (a) Variance of the displacements,  $\langle ([\Delta \mathbf{r}(t) - \mathbf{U}^{(0)}t]^2)$ , for different wavelengths  $\lambda/a$ ,  $h(0)/a = 0.2$ ,  $\epsilon = 0.1$ , and  $\mathbf{F} = F\mathbf{e} = F(\cos \pi/4, \sin \pi/4, 0)^T$ . Over the simulation horizon the sphere has translated  $\sim 60 \times a$  along the force. Results are obtained by averaging over  $10^3$  trajectories along different surface realizations [i.e., Eq. (5) with random  $\alpha_{nm}, \beta_{nm}$  ( $N = 20$ )]. Error bars remain smaller than the symbol size. Inset: Variance parallel (||), transverse (⊥), and perpendicular (z) to the force for  $\lambda/a = 2$ . (b), (c) Distributions of the displacements at subsequent times  $t_i$  (blue, red, and black correspond to the smallest, intermediate, and largest  $t_i$ ) for  $\lambda/a = 2$ . (b)  $\Delta h$  and (c)  $\Delta r_{\perp}$  relative to  $\Delta r_{\parallel} - \langle \Delta r_{\parallel} \rangle$  with  $\langle \Delta r_{\parallel} \rangle = U_{\parallel}t_i$ . The ellipses enclose 95% of the displacements.

The rotational velocity fluctuations display nonmonotonic behaviors where  $\langle (\Omega_{\perp}^{(1)})^2 \rangle$  saturates towards a plateau at large  $\lambda$  [Fig. 2(c)], which can be explained by the same physical mechanisms as introduced before. However,  $\langle (\Omega_{\parallel}^{(1)})^2 \rangle$  exhibits a bimodal shape with a local minimum at intermediate  $\lambda$ , where the flow reflected from nearby surface bumps prevents the sphere from rotating.

*Particle sedimentation near a rough wall.* We calculate particle trajectories by numerically integrating the equation of motion,  $\dot{\mathbf{r}}(t) = \mathbf{U} = \mathbf{U}^{(0)} + \epsilon \mathbf{U}^{(1)}$ , where  $\mathbf{r} = (r_{\parallel}, h)^T = r_{\parallel}\mathbf{e}_{\parallel} + r_{\perp}\mathbf{e}_{\perp} + h\mathbf{e}_z$ . We note that lubrication forces prevent the particle from touching  $S_0$ . The system displays two characteristic timescales: the time the sphere requires for (1)  $\tau_{\lambda} = \lambda/U_{\parallel}$  passing by a surface bump of wavelength  $\lambda$  along the force direction and (2)  $\tau = a/\langle (\epsilon \mathbf{U}^{(1)})^2 \rangle^{1/2}$  to move its radius due to hydrodynamic coupling with the surface texture. We find that by averaging over many surface realizations the particle displacement near a rough wall reduces to that near a planar wall,  $\langle \Delta \mathbf{r}(t) \rangle = \mathbf{U}^{(0)}t$  with  $\Delta \mathbf{r}(t) = \mathbf{r}(t) - \mathbf{r}(0)$ .

The impact of surface roughness becomes apparent in the variance of the displacements [Fig. 3(a)], which increases quadratically at short times  $t \lesssim \tau_{\lambda}$  as the sphere sediments by the first surface heterogeneity,  $\langle [\Delta \mathbf{r}(t) - \mathbf{U}^{(0)}t]^2 \rangle \simeq \langle (\epsilon \mathbf{U}^{(1)})^2 \rangle t^2$ . This regime is followed by a superdiffusive regime at  $t \sim \tau_{\lambda}$ , which reflects that while sedimenting near the textured surface the particles move around and up or down the underlying obstacles. By inspecting the individual contributions [Fig. 3(a) inset], we find that the mean-square displacement (MSD) for the perpendicular motion,  $\langle [\Delta h(t)]^2 \rangle$ , saturates towards a plateau at long times,  $t \gtrsim \tau_{\lambda}$ . This result indicates that transport towards and away from the wall is confined within a fluid layer near the surface, which is determined by  $h(0)$  and  $\lambda$ . This response means that the fundamental requirement of reversibility in Stokes flow is preserved. The MSDs in the transverse direction,  $\langle [\Delta r_{\perp}(t)]^2 \rangle$ , exhibit a plateau at intermediate times which indicates that subsequent obstacles bring the particle back to its initial position, so that over the simulation horizon the particle has merely displaced  $\sim 0.02a$  away from it. This could be due to the periodic nature of the surface structure, which causes, e.g., trajectories around obstacles that display fore-and-aft symmetries.

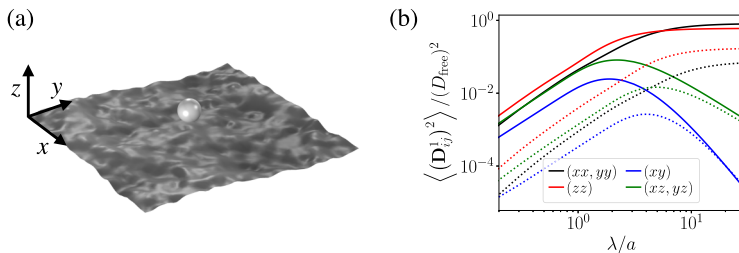


FIG. 4. (a) Schematic of a sphere diffusing near a rough surface. (b) Variance of the roughness-induced diffusivities,  $\langle (\mathbf{D}_{ij}^{(1)})^2 \rangle$ , as a function of  $\lambda/a$  for  $h/a = 0.1, 0.5$  (solid/dashed lines). The diffusivity in bulk is  $D_{\text{free}} = k_B T / (6\pi\mu a)$ .

At long times,  $t \gtrsim \tau_\lambda$ , the variance exhibits again a ballistic increase [Fig. 3(a)]. The direct contribution due to transverse and perpendicular motions is negligible, yet, due to that motion, the settling velocity changes and contributes to the variance of the displacements. Although all particles have started at the same distance  $h(0)$ , due to the underlying surface structure, some particles sediment on average at a distance  $h^* \lesssim h(0)$  closer to the surface and others farther away  $h^* \gtrsim h(0)$ , so that they display slower,  $\mathbf{U}^{(0)}(h^*) \lesssim \mathbf{U}^{(0)}[h(0)]$ , or faster settling velocities,  $\mathbf{U}^{(0)}(h^*) \gtrsim \mathbf{U}^{(0)}[h(0)]$ . Thus, particles that are closer to the surface displace less than average displacements  $\Delta r_{\parallel} \lesssim \langle \Delta r_{\parallel} \rangle$  while others sediment a longer distance than average,  $\Delta r_{\parallel} \gtrsim \langle \Delta r_{\parallel} \rangle$  [Fig. 3(b)]. Our simulations show that these effects generate a distribution of particle displacements along the force direction of width  $\propto t^2$ . Moreover, particles that sediment closer to the surface displace farther along the direction transverse to the force [Fig. 3(c)]. Yet, the transverse displacements remain rather small for the times considered,  $|\Delta r_{\perp}| \lesssim 0.1a$ .

*Remark on diffusion.* We note that the hydrodynamic mobility of the sphere is related to the diffusivity of a Brownian particle via the Stokes-Einstein relation  $\mathbf{D} = k_B T \mathbf{M}_{UF}$ , where  $k_B$  denotes the Boltzmann constant and  $T$  temperature. While a planar wall leads to a well-characterized anisotropic diffusion, where diffusion perpendicular to it is impeded more strongly than parallel motion [38], a rough surface generates additional, complex spatial dependence of the diffusivities [Fig. 4(a)]. The fluctuations of the roughness-induced diffusivities,  $\langle (\mathbf{D}_{ij}^{(1)})^2 \rangle = (k_B T)^2 \langle [(\mathbf{M}_{UF}^{(1)})_{ij}]^2 \rangle$ , along the principal axes, parallel  $[(xx), (yy)]$  and perpendicular to the surface  $(zz)$ , increase with  $\lambda$  and saturate towards a plateau [Fig. 4(b)]. The rough surface generates correlated motion encoded in the off-diagonal components  $[(xy), (xz), (yz)]$  that vary nonmonotonically with  $\lambda$ . The underlying physics has been rationalized earlier. For random rough surfaces diffusivities parallel to the surface coincide  $\langle (D_{xx}^{(1)})^2 \rangle = \langle (D_{yy}^{(1)})^2 \rangle$  and thus  $\langle (D_{xz}^{(1)})^2 \rangle = \langle (D_{yz}^{(1)})^2 \rangle$ .

*Conclusion.* We have presented an analytical expression for the mobility of a sphere near a textured surface and studied particle sedimentation near a random, rough wall. Our results show that hydrodynamic interactions between the particle and the surface roughness induce particle translation perpendicular and transverse to the force at velocities that depend nonmonotonically on the wavelength of the surface. This motion generates a quadratic increase in the variance of the displacements at long times along the force direction, as particles closer to the surface sediment significantly slower than particles that are farther away. These results are reminiscent of earlier predictions on force-induced dispersion of Brownian particles in heterogeneous media [39], yet they rely on different mechanisms, i.e., hydrodynamic interactions of non-Brownian particles with random, rough surfaces.

Our findings relate statistical transport features of sedimenting non-Brownian particles to the random nature of nearby surface structures that are produced by hydrodynamic coupling. We anticipate that our predictions will allow the noninvasive inference of surface properties by monitoring the transport of particles near rough surfaces, in the same spirit as particle suspensions have been used to quantify the effect of slip heterogeneities in channels [40] or diffusivities of

Brownian tracers have provided measures of surface slippage [41,42]. Specifically, measurement of the particle displacements or quantitative extraction of its velocity fluctuations encode information about the characteristic wavelength and amplitude of the surface structure. The roughness-induced mobilities hold for arbitrary surface shapes, which include other random rough surface models or grooved, periodic structures. The latter could serve as input for novel particle separation methods [43] that harness the nonmonotonic behavior of particle velocities near textured walls.

Furthermore, our predictions for the particle diffusivities can be employed to explore diffusion near corrugated substrates [38] and thereby draw a connection to coarse-grained theories [44,45]. Our theory can immediately be extended to derive roughness-induced velocities of microswimmers and thus elucidate the hydrodynamic effect of textured surfaces on active transport [46–49].

*Acknowledgments.* C.K. acknowledges support from the Austrian Science Fund (FWF) via the Erwin Schrödinger fellowship (Grant No. J4321-N27). The work was supported by NSF MCB-1853602 (H.A.S.). L.Z. thanks the Swedish Research Council for a VR International Postdoc Grant (2015-06334) and NUS for the startup grant (R-265-000-696-133).

- 
- [1] Q. Wang, D. H. Tolley, D. A. LeFebvre, and M. L. Lee, Analytical equilibrium gradient methods, *Anal. Bioanal. Chem.* **373**, 125 (2002).
  - [2] P. Sajeesh and A. K. Sen, Particle separation and sorting in microfluidic devices: A review, *Microfluid. Nanofluid.* **17**, 1 (2014).
  - [3] M. Garcia, *Sedimentation Engineering* (American Society of Civil Engineers, Reston, VA, 2008).
  - [4] P. N. Segrè, E. Herbolzheimer, and P. M. Chaikin, Long-Range Correlations in Sedimentation, *Phys. Rev. Lett.* **79**, 2574 (1997).
  - [5] S.-Y. Tee, P. J. Mucha, L. Cipelletti, S. Manley, M. P. Brenner, P. N. Segre, and D. A. Weitz, Nonuniversal Velocity Fluctuations of Sedimenting Particles, *Phys. Rev. Lett.* **89**, 054501 (2002).
  - [6] A. J. C. Ladd, Effects of Container Walls on the Velocity Fluctuations of Sedimenting Spheres, *Phys. Rev. Lett.* **88**, 048301 (2002).
  - [7] S. Heitkam, Y. Yoshitake, F. Toquet, D. Langevin, and A. Salonen, Speeding up of Sedimentation Under Confinement, *Phys. Rev. Lett.* **110**, 178302 (2013).
  - [8] E. Bonaccorso, H.-J. Butt, and V. S. J. Craig, Surface Roughness and Hydrodynamic Boundary Slip of a Newtonian Fluid in a Completely Wetting System, *Phys. Rev. Lett.* **90**, 144501 (2003).
  - [9] C. Kunert, J. Harting, and O. I. Vinogradova, Random-Roughness Hydrodynamic Boundary Conditions, *Phys. Rev. Lett.* **105**, 016001 (2010).
  - [10] K. Kamrin, M. Z. Bazant, and H. A. Stone, Effective slip boundary conditions for arbitrary periodic surfaces: The surface mobility tensor, *J. Fluid Mech.* **658**, 409 (2010).
  - [11] T. Lee, E. Charrault, and C. Neto, Interfacial slip on rough, patterned and soft surfaces: A review of experiments and simulations, *Adv. Colloid Interface Sci.* **210**, 21 (2014).
  - [12] R. Assoudi, K. Lamzoud, and M. Chaoui, Influence of the wall roughness on a linear shear flow, *FME Trans.* **46**, 272 (2018).
  - [13] S. H. Rad and A. Najafi, Hydrodynamic interactions of spherical particles in a fluid confined by a rough no-slip wall, *Phys. Rev. E* **82**, 036305 (2010).
  - [14] R. Assoudi, M. Chaoui, F. Feuillebois, and H. Allouche, Motion of a spherical particle along a rough wall in a shear flow, *Z. Angew. Math. Phys.* **69**, 112 (2018).
  - [15] L. R. Huang, E. C. Cox, R. H. Austin, and J. C. Sturm, Continuous particle separation through deterministic lateral displacement, *Science* **304**, 987 (2004).
  - [16] J. A. Davis, D. W. Inglis, K. J. Morton, D. A. Lawrence, L. R. Huang, S. Y. Chou, J. C. Sturm, and R. H. Austin, Deterministic hydrodynamics: Taking blood apart, *Proc. Natl. Acad. Sci. U.S.A.* **103**, 14779 (2006).

- [17] J. McGrath, M. Jimenez, and H. Bridle, Deterministic lateral displacement for particle separation: A review, *Lab Chip* **14**, 4139 (2014).
- [18] T. M. Squires and T. G. Mason, Fluid mechanics of microrheology, *Annu. Rev. Fluid Mech.* **42**, 413 (2010).
- [19] R. N. Zia, Active and passive microrheology: Theory and simulation, *Annu. Rev. Fluid Mech.* **50**, 371 (2018).
- [20] M. E. O’Neill and K. Stewartson, On the slow motion of a sphere parallel to a nearby plane wall, *J. Fluid Mech.* **27**, 705 (1967).
- [21] A. J. Goldman, R. G. Cox, and H. Brenner, Slow viscous motion of a sphere parallel to a plane wall – I Motion through a quiescent fluid, *Chem. Eng. Sci.* **22**, 637 (1967).
- [22] W. Russel, E. Hinch, L. Leal, and G. Tieffenbruck, Rods falling near a vertical wall, *J. Fluid Mech.* **83**, 273 (1977).
- [23] W. H. Mitchell and S. E. Spagnolie, Sedimentation of spheroidal bodies near walls in viscous fluids: Glancing, reversing, tumbling and sliding, *J. Fluid Mech.* **772**, 600 (2015).
- [24] P. Vasseur and R. G. Cox, The lateral migration of spherical particles sedimenting in a stagnant bounded fluid, *J. Fluid Mech.* **80**, 561 (1977).
- [25] L. Becker, G. McKinley, and H. A. Stone, Sedimentation of a sphere near a plane wall: Weak non-Newtonian and inertial effects, *J. Non-Newton. Fluid* **63**, 201 (1996).
- [26] B. Rallabandi, N. Oppenheimer, M. Y. B. Zion, and H. A. Stone, Membrane-induced hydroelastic migration of a particle surfing its own wave, *Nat. Phys.* **14**, 1211 (2018).
- [27] A. V. Belyaev, Hydrodynamic repulsion of spheroidal microparticles from micro-rough surfaces, *PLoS One* **12**, 1 (2017).
- [28] F. Charru, E. Larrieu, J.-B. Dupont, and R. Zenit, Motion of a particle near a rough wall in a viscous shear flow, *J. Fluid Mech.* **570**, 431 (2007).
- [29] G. B. Jeffery, On the steady rotation of a solid of revolution in a viscous fluid, *Proc. London Math. Soc.* **s2\_14**, 327 (1915).
- [30] H. Brenner, The slow motion of a sphere through a viscous fluid towards a plane surface, *Chem. Eng. Sci.* **16**, 242 (1961).
- [31] W. R. Dean and M. E. O’Neill, A slow motion of viscous liquid caused by the rotation of a solid sphere, *Mathematika* **10**, 13 (1963).
- [32] M. E. O’Neill, A slow motion of viscous liquid caused by a slowly moving solid sphere, *Mathematika* **11**, 67 (1964).
- [33] L. G. Leal, *Advanced Transport Phenomena: Fluid Mechanics and Convective Transport Processes*, Vol. 7 (Cambridge University Press, Cambridge, U.K., 2007).
- [34] H. Masoud and H. A. Stone, The reciprocal theorem in fluid dynamics and transport phenomena, *J. Fluid Mech.* **879**, P1 (2019).
- [35] See Supplemental Material at <http://link.aps.org/supplemental/10.1103/PhysRevFluids.5.082101> for details on the theory and numerics, which includes Refs. [50–55].
- [36] S. Kim and S. J. Karrila, *Microhydrodynamics: Principles and Selected Applications* (Courier Corporation, North Chelmsford, MA, 2013).
- [37] N. Savva, S. Kalliadasis, and G. A. Pavliotis, Two-Dimensional Droplet Spreading Over Random Topographical Substrates, *Phys. Rev. Lett.* **104**, 084501 (2010).
- [38] X. Bian, C. Kim, and G. E. Karniadakis, 111 years of Brownian motion, *Soft Matter* **12**, 6331 (2016).
- [39] T. Guérin and D. S. Dean, Force-Induced Dispersion in Heterogeneous Media, *Phys. Rev. Lett.* **115**, 020601 (2015).
- [40] A.-L. Vayssade, C. Lee, E. Terriac, F. Monti, M. Cloitre, and P. Tabeling, Dynamical role of slip heterogeneities in confined flows, *Phys. Rev. E* **89**, 052309 (2014).
- [41] E. Lauga and T. M. Squires, Brownian motion near a partial-slip boundary: A local probe of the no-slip condition, *Phys. Fluids* **17**, 103102 (2005).
- [42] L. Joly, C. Ybert, and L. Bocquet, Probing the Nanohydrodynamics at Liquid-Solid Interfaces using Thermal Motion, *Phys. Rev. Lett.* **96**, 046101 (2006).



- [43] E. S. Asmolov, A. L. Dubov, T. V. Nizkaya, A. J. C. Kuehne, and O. I. Vinogradova, Principles of transverse flow fractionation of microparticles in superhydrophobic channels, [Lab Chip](#) **15**, 2835 (2015).
- [44] E. Reister-Gottfried, S. M. Leitenberger, and U. Seifert, Hybrid simulations of lateral diffusion in fluctuating membranes, [Phys. Rev. E](#) **75**, 011908 (2007).
- [45] A. Naji and F. L. H. Brown, Diffusion on ruffled membrane surfaces, [J. Chem. Phys.](#) **126**, 235103 (2007).
- [46] D. Takagi, J. Palacci, A. B. Braunschweig, M. J. Shelley, and J. Zhang, Hydrodynamic capture of microswimmers into sphere-bound orbits, [Soft Matter](#) **10**, 1784 (2014).
- [47] T. Ostapenko, F. J. Schwarzendahl, T. J. Bøddeker, C. T. Kreis, J. Cammann, M. G. Mazza, and O. Bäumchen, Curvature-Guided Motility of Microalgae in Geometric Confinement, [Phys. Rev. Lett.](#) **120**, 068002 (2018).
- [48] G. Frangipane, G. Vizsnyiczai, C. Maggi, R. Savo, A. Sciortino, S. Gigan, and R. Di Leonardo, Invariance properties of bacterial random walks in complex structures, [Nat. Commun.](#) **10**, 2442 (2019).
- [49] S. Makarchuk, V. C. Braz, N. A. M. Araújo, L. Ciric, and G. Volpe, Enhanced propagation of motile bacteria on surfaces due to forward scattering, [Nat. Commun.](#) **10**, 4110 (2019).
- [50] R. G. Cox and H. Brenner, The slow motion of a sphere through a viscous fluid towards a plane surface—II Small gap widths, including inertial effects, [Chem. Eng. Sci.](#) **22**, 1753 (1967).
- [51] J. R. Blake and A. T. Chwang, Fundamental singularities of viscous flow, [J. Eng. Math.](#) **8**, 23 (1974).
- [52] C. Pozrikidis, *Boundary Integral and Singularity Methods for Linearized Viscous Flow* (Cambridge University Press, Cambridge, U.K., 1992).
- [53] C. Pozrikidis, *A Practical Guide to Boundary Element Methods with the Software Library BEMLIB* (CRC Press, Boca Raton, FL, 2002).
- [54] L. Zhu, E. Lauga, and L. Brandt, Low-Reynolds-number swimming in a capillary tube, [J. Fluid Mech.](#) **726**, 285 (2013).
- [55] L. Zhu and F. Gallaire, Bifurcation Dynamics of a Particle-Encapsulating Droplet in Shear Flow, [Phys. Rev. Lett.](#) **119**, 064502 (2017).